Clinical Cancer Research

BAI1 Orchestrates Macrophage Inflammatory Response to HSV Infection—Implications for Oncolytic Viral Therapy

Chelsea Bolyard[1,2], W. Hans Meisen[1,2], Yeshavanth Banasavadi-Siddegowda[1,2], Jayson Hardcastle[1], Ji Young Yoo[1,2], Eric S. Wohleb[3], Jeffrey Wojton[1], Jun-Ge Yu[2,4], Samuel Dubin[1,2], Maninder Khosla[2,4], Bo Xu[2], Jonathan Smith[1], Christopher Alvarez-Breckenridge[1,2], Pete Pow-anpongkul[1,2], Flavia Pichiorri[5], Jianying Zhang[2,6], Matthew Old[2,4], Dan Zhu[7], Erwin G. Van Meir[7], Jonathan P. Godbout[2,3], Michael A. Caligiuri[2], Jianhua Yu[2], and Balveen Kaur[1,2]

Abstract

Purpose: Brain angiogenesis inhibitor (BAI1) facilitates phagocytosis and bacterial pathogen clearance by macrophages; however, its role in viral infections is unknown. Here, we examined the role of BAI1, and its N-terminal cleavage fragment (Vstat120) in antiviral macrophage responses to oncolytic herpes simplex virus (oHSV).

Experimental Design: Changes in infiltration and activation of monocytic and microglial cells after treatment of glioma-bearing mice brains with a control (rHSVQ1) or Vstat120-expressing (RAMBO) oHSV was analyzed using flow cytometry. Co-culture of infected glioma cells with macrophages or microglia was used to examine antiviral signaling. Cytokine array gene expression and Ingenuity Pathway Analysis (IPA) helped evaluate changes in macrophage signaling in response to viral infection. TNFα-blocking antibodies and macrophages derived from *Bai1*$^{-/-}$ mice were used.

Results: RAMBO treatment of mice reduced recruitment and activation of macrophages/microglia in mice with brain tumors, and showed increased virus replication compared with rHSVQ1. Cytokine gene expression array revealed that RAMBO significantly altered the macrophage inflammatory response to infected glioma cells via altered secretion of TNFα. Furthermore, we showed that BAI1 mediated macrophage TNFα induction in response to oHSV therapy. Intracranial inoculation of wild-type/RAMBO virus in *Bai1*$^{-/-}$ or wild-type non–tumor-bearing mice revealed the safety of this approach.

Conclusions: We have uncovered a new role for BAI1 in facilitating macrophage anti-viral responses. We show that arming oHSV with antiangiogenic Vstat120 also shields them from inflammatory macrophage antiviral response, without reducing safety. *Clin Cancer Res; 23(7); 1809–19. ©2016 AACR.*

Introduction

Glioblastoma is the most common primary malignant brain tumor, with a median survival of less than 15 months from diagnosis (1). Current standard of care combines surgical resection, with radiation and chemotherapy, but even with this aggressive first line of therapy, most patients relapse with refractive and resistant disease (2). Five-year survival for adults (>40 years) remains less than 10%. Thus, there is an urgent need to develop novel therapeutics to fight this disease. HSV-1–derived oncolytic viruses (oHSV) are one such novel promising therapeutic strategy, which use genetically modified viruses to exploit weakened protein kinase R (PKR) response in malignant cells, to specifically replicate and destroy tumors (3). First-generation attenuated viruses have proven safe in clinical trials, and have paved the way for second-generation armed viruses that can deliver a therapeutic payload to the tumor microenvironment (4). T-Vec (tamilogenelaherpavec; IMLYGIC) is an attenuated second-generation oHSV that encodes GM-CSF, and was recently approved for use in unresectable metastatic melanoma (5).

We have recently described the generation and antitumor efficacy of an oHSV-expressing antiangiogenic Vstat120, called RAMBO (rapid anti-angiogenesis mediated by oncolytic virus; ref. 6). Vstat120 is the extracellular fragment of brain angiogenesis inhibitor 1 (BAI1/ADGRB1), an adhesion G-protein–coupled receptor (GPCR) primarily expressed in the brain. The expression of this protein is reduced in several solid tumors including glioblastoma, colorectal cancer, pulmonary adenocarcinoma, and

[1]Department of Neurological Surgery, The Ohio State University College of Medicine, Columbus, Ohio. [2]The James Comprehensive Cancer Center, The Ohio State University, Columbus, Ohio. [3]Department of Neuroscience, The Ohio State University Wexner Medical Center, Columbus, Ohio. [4]Department of Otolaryngology, Head and Neck Surgery, The Ohio State University College of Medicine, Columbus, Ohio. [5]Department of Hematology, City of Hope Cancer Center, Duarte, California. [6]Department of Biomedical Informatics, Center for Biostatistics, The Ohio State University College of Medicine, Columbus, Ohio. [7]Departments of Neurosurgery and Hematology and Medical Oncology, School of Medicine and Winship Cancer Institute, Emory University, Atlanta, Georgia.

Note: Supplementary data for this article are available at Clinical Cancer Research Online (http://clincancerres.aacrjournals.org/).

C. Bolyard and W.H. Meisen contributed equally to this article.

Corresponding Author: Balveen Kaur, Department of Neurological Surgery, The Ohio State University, 385-B, OSUCCC, 410 West 12th Avenue Columbus, OH 43210. Phone: 614-292-3984; Fax: 614-688-4882; E-mail: Balveen.Kaur@osumc.edu

doi: 10.1158/1078-0432.CCR-16-1818

Translational Relevance

Brain-specific angiogenesis inhibitor 1 (BAI1/ADGRB1) is an adhesion G-protein–coupled receptor that serves as a scavenger receptor on macrophages implicated in bacterial and apoptotic cell clearance. Here we report that BAI1 directs macrophage-mediated virus clearance by inducing production of antiviral TNFα. This results in clearance of oncolytic HSV-1 (oHSV) viruses from a tumor and hinders oncolytic viral therapy. Proteolysis of BAI1's N-terminus generates a 120-kDa fragment called vasculostatin (Vstat120) with potent antiangiogenic effects. Here we show that Vstat120-armed oHSV are also shielded from BAI1-mediated antiviral signaling, resulting in reduced tumoral inflammation and increased viral propagation *in vivo*. Furthermore, our results show that while attenuating antiviral responses by macrophages/microglia leads to increased OV replication in vivo, this approach remains safe upon intracranial inoculation in animals. This study supports further development of this strategy for clinical development.

others, suggesting its loss may be of significance in tumor progression or growth (7–11). Consistent with this, Vstat120 binds to CD36 on endothelial cells, leading to their apoptosis (12). The potent antiangiogenic effects of Vstat120 result in reduced tumor growth and angiogenesis in several preclinical studies when tumor cells overexpress it (13).

Apart from astrocytes and neurons, BAI1 is also expressed on macrophages and microglia (14–16), where it mediates a variety of functions including phagocytosis, and clearance of apoptotic cells via its ability to recognize phosphatidylserine (14, 16, 17). As a pattern recognition receptor, its expression on macrophages is important for the identification of Gram-negative bacteria through their surface lipopolysaccharides, and activation of proinflammatory immune responses (18). The antiangiogenic and phagocytic functions of BAI1 involve the five thrombospondin type I repeats (TSR) present on the extracellular domain of the receptor (14, 18), thus implying that Vstat120 might modulate this function. The role of BAI1 or Vstat120 in orchestrating antiviral macrophage innate responses has not been previously investigated.

Macrophages mediate an innate immune response against viral infection that antagonizes oHSV replication. This response is thought to be one of the major factors that limits virus spread, and reduces tumor destruction through direct viral oncolysis (19–22). Macrophages can directly uptake viruses through endocytosis, or reduce viral replication through secretion of antiviral cytokines (22, 23). Several studies have shown that blocking microglia and infiltrating macrophages can significantly increase oHSV therapeutic efficacy, and these strategies may be translatable to patients (24–29). Given the role of BAI1 in phagocytosis and bacterial clearance, we hypothesize that it might choreograph an antiviral defense response in macrophages, and that Vstat120 its soluble extracellular fragment could interfere with this function.

Materials and Methods

Cell lines

LN229, X12v2, U87ΔEGFR, and U251-T2 human glioma cell lines and Vero cells were maintained in DMEM supplemented with 10% FBS. U251-T2/T3 were created by serially passaging U251MG cells in mice two or three times, respectively. Monkey kidney epithelial-derived Vero cells and U87ΔEGFR human glioma cells were obtained from E.A. Chiocca (Ohio State University, Columbus, OH). X12v2 cells were obtained from Mayo Clinic, and maintained in DMEM supplemented with 2% FBS on adherent flasks. Murine BV2 microglia were maintained in DMEM supplemented with 2% FBS. Murine RAW264.7 macrophages were received from S. Tridandapani (Ohio State University, Columbus, Ohio), and were grown in RPMI supplemented with 10% FBS. All human cells were routinely authenticated through the University of Arizona Genetics Core via STR profiling and maintained below passage 50 after STR profiling. All cells were routinely monitored for changes in morphology and growth rate. All cells are routinely tested for mycoplasma. All cells were incubated at 37°C in an atmosphere with 5% carbon dioxide, and maintained with 100 U/mL penicillin, and 0.1 mg/mL streptomycin.

Viruses and virus replication assay

Genetic composition of rHSVQ1 and RAMBO viruses were previously described (6, 31), and their titers determined on Vero cells via a standard plaque-forming unit (PFU) assay (32).

Co-culture assays

Glioma cells were infected with virus at a multiplicity of infection (MOI) of 1 or 2 as indicated in DMEM supplemented with 0.05% FBS for 1 hour and then washed with PBS to remove unbound virus. Infected cells were then overlaid with microglia or macrophages (at 2:1 ratio of macrophages/microglia to glioma cells) for 12 hours; samples were collected pre-virus burst. For TNFα-blocking antibody assays, 1,800 ng/mL of mouse TNFα-neutralizing antibody (D2H4; Cell Signaling Technology) or an isotype control were used. For mouse Inflammatory Cytokines & Receptors PCR Array, Quantitative mRNA expression analysis of 84 murine inflammatory cytokines and chemokines was performed using the Mouse Inflammatory Cytokines & Receptors RT2 Profiler PCR array (Cat. no. PAMM-011Z; QIAGEN, SABioscience Corporation, Frederick, MD, USA) per manufacturer's instruction. Total RNA was collected from co-cultures as described above using RNeasy Mini Kit (QIAGEN). cDNA was synthesized from 1ug DNase-treated RNA by reverse transcription using SuperScript II Reverse Transcriptase (ThermoFisher Scientific). PCR array analysis was performed according to the manufacturer protocol with the RT2 Real-Time SYBR Green PCR Master Mix (SABioscience Corporation). mRNA expression for each gene was normalized to control housekeeping gene beta-actin, and analyzed using the SABiosciences PCR Array analysis software (sabiosciences.com). Results were considered significant when relative mRNA expression was 1.5-fold higher or lower than that of the uninfected samples. P-values ≤ 0.05 were considered to be significant.

Isolation of tumor-associated brain microglia and macrophages

Microglia and macrophage populations were isolated for flow cytometry analysis from murine brain homogenates as previously described (22). Briefly, the tumor-bearing hemispheres of mice brains were dissected, and microglia/macrophage populations were collected via Percoll isolation from the interphase between the 70% and 50% Percoll gradient layers.

Primary murine bone marrow–derived macrophage generation

Bai1$^{+/-}$heterozygote breeding pairs were bred and wild-type and knock out mice identified by PCR as described previously (33). Bone marrow–derived macrophages were isolated as previously described (34). Briefly, the tibia and femurs of euthanized mice were flushed with PBS several times to remove bone marrow cells. Cells were centrifuged and plated in RPMI medium supplemented with 10% FBS and 1% penicillin/streptomycin. Murine macrophage colony stimulating factor (20 ng/mL; R&D Systems) and 10 μg/mL of polymyxin B (Calbiochem/EMD Millipore) were added to the cultures. Cells were allowed to mature for 8 days before use.

Microglia and macrophage antibody staining

Staining of surface antigens were performed as previously described (35, 36). Briefly, Fc receptors were blocked with anti-CD16/CD32 antibody (eBioscience). Cells were then incubated with the appropriate antibodies: CD45, CD11b, MHCII, CD86, LY6C, and CD206 (eBioscience) for 45 minutes. Cells were resuspended in FACS buffer (2% FBS in HBSS with 1 mg/mL sodium azide) for analysis. Nonspecific binding was assessed via isotype-matched antibodies. Antigen expression was determined using a Becton-Dickinson FACS Caliber four-color cytometer. Ten thousand events were recorded for each sample and isotype matched-conjugate. Data was analyzed using FlowJo software (FlowJo, LLC).

Animal surgery

All animal experiments were performed in accordance with the Subcommittee on Research Animal Care of The Ohio State University guidelines, and were approved by the institutional review board. Intracranial surgeries were performed as previously described with stereotactic implantation of 100,000 U87ΔEGFR in nude mice (32). Tumors were treated with HBSS/PBS, rHSVQ1, or RAMBO virus (1×10^5 PFU/mouse) at the location of tumor implantation. Tumor-bearing hemispheres were collected by gross dissection 3 days after treatment, or as indicated. For safety studies, we used female BALB/C mice (∼6 weeks of age) or *Bai1* wild-type or knockout C57/Bl/6 mice (male and female littermates; ref. 33). Virus (F strain or RAMBO) was injected into naïve brains at indicated doses. Weight was recorded to the nearest gram, and the mice were euthanized upon reaching early removal criteria.

Statistical analysis

Student *t* test, one-way ANOVA with Bonferroni multiple comparison *post hoc* tests, or two-way ANOVA with Tukey correction for multiple comparisons were used to analyze changes in cell killing, viral plaque-forming assays, gene expression, and flow cytometry assays. Statistical analyses were performed with the use of GraphPad Prism software (version 5.01) or by a biostatistician. A *P* value of ≤ 0.05 was considered statistically significant. Derived *P* values are identified as *, $P \leq 0.05$; **, $P \leq 0.01$; ***, $P \leq 0.001$; ****, $P \leq 0.0001$. For the cytokine gene expression analysis, CT scores were processed and analyzed by QIAGEN web portal directly (Qiagen/SABiosciences; GeneGlobe Data Analysis Center). Differentially expressed genes were selected by a fold change greater than 1.5 and *P* value less than 0.05.

Results

Impact of RAMBO on infiltration and activation of macrophages and microglia in intracranial tumors

To examine the effect of macrophage/microglia responses to oHSV infection with or without Vstat120, we treated mice with established intracranial gliomas with PBS, rHSVQ1 (control oHSV), or RAMBO (oHSV-expressing Vstat120). Three days after treatment, we analyzed tumor-bearing hemispheres for infiltrating monocytic macrophages ($CD11b^{hi}/CD45^{hi}$) and microglia ($CD11b^{+}/CD45^{int}$) cells by flow cytometry. Consistent with previous studies (22), rHSVQ1 infection resulted in a significant increase in macrophage infiltration, compared with PBS injection control (PBS, 3.41% vs. rHSVQ1, 25.17%; $P \leq 0.001$; Fig. 1A). Interestingly, RAMBO treatment resulted in a significant reduction in virus-induced macrophage infiltration, compared with rHSVQ1 (rHSVQ1, 25.17% vs. RAMBO, 5.60%; $P \leq 0.001$; Fig. 1A).

To further evaluate the activation status of the tumor-infiltrating macrophages, we stained them for antigen-presenting molecule MHCII, activation marker Ly6c, pattern recognition receptor CD206, and T-cell–costimulatory signal CD86. As previously reported, rHSVQ1 treatment increased expression of activation markers on macrophages and microglia (Fig. 1B and C; light gray bars; ref. 22). Surprisingly, we saw a reduction in expression of activation markers on both infiltrating macrophages and resident microglia in RAMBO-treated tumors (Fig. 1B and C; dark gray bars). Combined, these data show that RAMBO infection is associated with dramatically reduced macrophage infiltration, and that these cells are in a lower immune activation state. To address the generalizability of these results, we performed a similar experiment using a murine model of Ewing sarcoma. Subcutaneous tumors were treated with rHSVQ1 or RAMBO, and tumor tissue was collected 3 days after virus treatment. Using IHC of tumor sections, we stained the tumors for $CD68^{+}$ cells, indicative of macrophages (Supplementary Fig. S1). Similar to results described above (Fig. 1), we found a robust decrease in macrophages in RAMBO-treated tumors (Supplementary Fig. S1, brown staining).

Impact of RAMBO on macrophage and microglial responses to oHSV

Because both macrophages and microglia are implicated in oncolytic virus clearance (22), we compared the effect of macrophages and microglia on rHSVQ1 or RAMBO replication in an *in vitro* coculture model. Human glioma cells infected with GFP-expressing oHSV were overlaid with murine microglia (BV2) or macrophages (RAW264.7; schematic in Fig. 2A). In the absence of macrophages or microglia, rHSVQ1 and RAMBO infected and replicated in glioma cells equally [Fig. 2B and C; (−), no overlay], and did not have productive replication in either macrophages or microglia alone (not shown). Flow cytometry analysis of tumor cells infected with GFP-expressing rHSVQ1 revealed a reduction in fluorescent cells in the presence of either BV2 or RAW cells (Fig. 2B, black bars). The number of GFP-positive (GFP^{+}) glioma cells infected with RAMBO was higher than that obtained with rHSVQ1 in the presence of macrophages, as well as microglia [Fig. 2B, black bars (rHSVQ1) vs. gray bars (RAMBO)]. Consistent with a reduction in infected tumor cells, addition of microglia or macrophages reduced the replication of both viruses, albeit to a lesser extent for RAMBO [Fig. 2C, black bars (rHSVQ1) vs. gray bars (RAMBO)]. In addition, Vstat120 expression by glioma cells cultured with HSVQ1-infected glioma cells did not affect virus

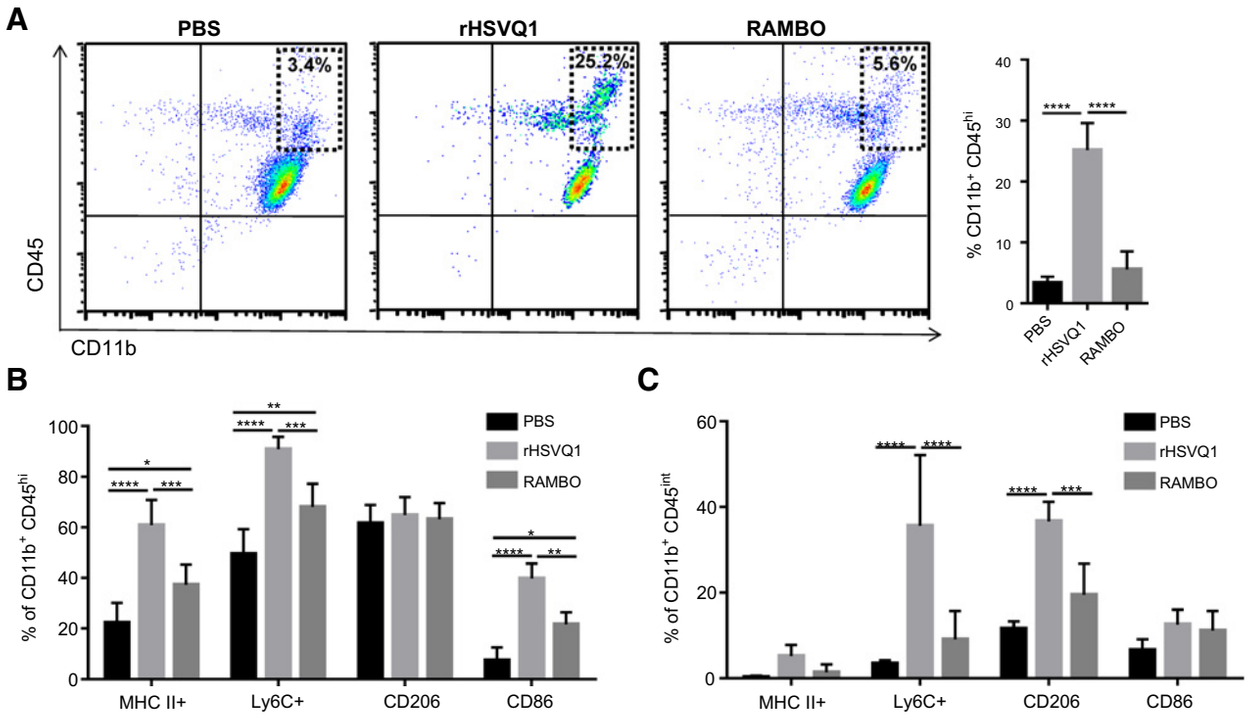

Figure 1.

Effect of RAMBO on macrophage and microglial response to oHSV therapy. Mice bearing intracranial U87ΔEGFR tumors treated with PBS, rHSVQ1 or RAMBO were sacrificed 3 days after treatment, and tumor-bearing hemispheres were analyzed for macrophage or microglia infiltration and activation by flow cytometry. **A,** Left, representative scatter plots showing CD11b$^+$/CD45$^+$ cells isolated from tumor-bearing hemispheres from mice. Dashed box, indicates CD11b^{hi}CD45^{hi} infiltrating monocytic macrophages. Right represents mean percentage of CD11b^{hi}CD45^{hi} of population from three independent experiments (mean ± SD). **B,** The percentage of CD11b^{hi}CD45^{hi} cells (infiltrating monocytic macrophages) staining positive for activation markers MHCII, Ly6C, CD206, and CD86. **C,** The percentage of CD11b$^+$CD45^{int} cells (microglia) staining positive for activation markers MHCII, Ly6C, CD206, and CD86. (*, $P \leq 0.05$; **, $P \leq 0.01$; ***, $P \leq 0.001$; ****, $P \leq 0.0001$).

replication. Coculture of Vstat120-expressing glioma cells with rHSVQ1-infected glioma before overlay with macrophages rescued virus replication inhibition by macrophages [Supplementary Fig. S2B, right (control glioma overlay) vs. left (Vstat120-expressing glioma overlay)]. Together, these findings show that macrophages/microglia suppress HSV-1 infection and replication in glioma cells in culture, and that the presence of Vstat120 in the secreted ECM rescues the effect of macrophage/microglia-mediated inhibition of OV replication.

To evaluate the *in vivo* significance of these results, we treated mice bearing established intracranial glioma with rHSVQ1 or RAMBO. At indicated time points after virus treatment, we measured viral ICP4 gene expression from tumor-bearing hemispheres (Fig. 2D). The peak of viral transgene expression occurred 7 days after oHSV treatment. At this time point, and over time, RAMBO showed significantly more replication in xenograft glioma model as compared with rHSVQ1 [rHSVQ1, 1.9-fold increase in *ICP4* gene expression on day 7 over baseline; RAMBO, 3.8-fold increase over baseline ($P \leq 0.001$)].

Reduced antiviral immune response from macrophages in response to RAMBO infection in glioma cells

The above results suggested that RAMBO could reduce macrophage antiviral signaling. To probe for changes in anti-viral immune signaling in macrophages, we used a mouse species-specific antiviral gene-expression RT-PCR array to tease out changes in macrophage transcripts when exposed to control or virally infected glioma cells in a co-culture system. Genes altered by >1.5-fold were considered changed. Volcano plots evidenced a clear induction of 65 out of the 84 antiviral genes represented on the array in macrophages cocultured with rHSVQ1-infected human glioma cells (Fig. 3A and B; left; Supplementary Table S1). Only 50 of these 65 cytokine genes were upregulated in macrophages cultured with RAMBO-infected glioma cells (Fig. 3A and B; middle; Supplementary Table S1). Comparison of the level of induction of these 50 mRNAs under either rHSVQ1 versus RAMBO-infected cell culture conditions, evidenced that 14 showed higher induction (>1.5-fold more) in the rHSVQ1-infected coculture (Fig. 3A and B; Supplementary Table S2). We then used Ingenuity Pathway Analysis (Fig. 3C), a software that uses algorithms to build networks based on the functional and biological connectivity of genes, to examine for connectivity between these 14 cytokines, and found convergence on canonical pathways associated with TNF receptor signaling (Fig. 3C). From this analysis, TNFα emerged as a major signaling node negatively regulated by RAMBO.

Reduced TNFα production from macrophages and microglia in response to RAMBO-infected tumor cells

To validate the IPA network prediction, we examined changes in TNFα gene expression by macrophages or microglia after

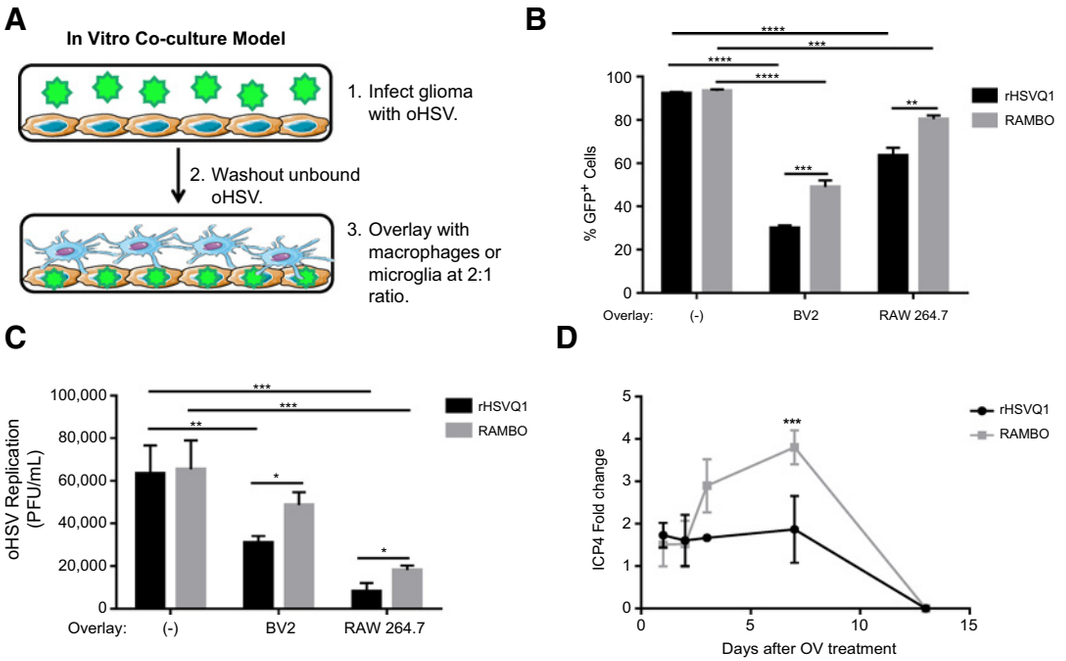

Figure 2.

Effect of macrophage and microglial cells on oHSV replication. **A,** Schematic of experimental design used: U251 glioma cells (brown) were infected with oHSV (rHSVQ1 or RAMBO; green) for an hour before unbound virus was washed away. Macrophages (RAW 264.7) or microglia (BV2) represented in blue were then overlaid onto infected tumor cells, at a 2:1 ratio. **B,** Changes in the percentage of GFP^+ infected tumor cells in the presence or absence of macrophage (RAW 264.7) or microglia (BV2) was measured by flow cytometry 12 hours after infection with the indicated virus. Data shown are mean percentage of GFP^+ tumor cells ($\pm$ SD) upon infection with the indicated virus ($n = 3$ samples/group). **C,** Changes in oHSV replication from infected tumor cells in the presence or absence of RAW or BV2 cells 12 hours after infection was measured by a standard plaque assay. Data shown are mean plaque-forming U/mL $\pm$ SD. **D,** Mice bearing intracranial U87ΔEGFR tumors treated with rHSVQ1 or RAMBO were sacrificed at indicated time points after treatment, and tumor-bearing hemispheres were analyzed for viral *ICP4* gene expression. (*, $P \leq 0.05$; **, $P \leq 0.01$; ***, $P \leq 0.001$; ****, $P \leq 0.0001$).

coculture with multiple different human glioma cell lines infected with rHSVQ1 or RAMBO. Briefly, the indicated human glioma cells were infected with either rHSVQ1 or RAMBO and then overlaid with murine microglia (BV2) or murine macrophages (RAW264.7). Changes in macrophage/microglia TNFα gene expression relative to uninfected cultures was assessed by quantitative RT-PCR using species-specific primers. Consistent with the cytokine array profile, macrophages and microglia cultured with RAMBO-infected glioma cells showed a significantly reduced induction of TNFα, compared with rHSVQ1 coculture (Fig. 4A).

To evaluate the *in vivo* significance of these results, we compared TNFα secretion in mice bearing intracranial tumors treated with rHSVQ1 or RAMBO. Briefly, mice bearing intracranial tumors were treated with the indicated virus 7 days after tumor cell implantation. Three days after treatment, mice were sacrificed and tumor-bearing hemispheres were harvested and lysed. Figure 4B shows a significant increase in murine TNFα after rHSVQ1 treatment, compared with untreated controls ($P \leq 0.001$), and a significantly less robust expression with RAMBO treatment relative to rHSVQ1 treatment ($P \leq 0.05$).

Effect of TNFα blockage on microglial response to oHSV

Collectively, our results show that increased replication of RAMBO *in vivo* correlates with: (i) reduced macrophage/microglial infiltration; (ii) reduced macrophage/microglial activation; and (iii) reduced TNFα production in response to infected tumor cells. TNFα is a pleiotropic cytokine upregulated in response to CNS infections and we have previously shown that it plays a key role in blocking oHSV efficacy (22). To determine whether induction of TNFα in macrophage/microglial cells plays a causal role in the differential viral replication efficacy in the coculture system, we compared rHSVQ1 and RAMBO replication efficacy in the presence or absence of TNFα-blocking antibody. As already observed above, RAMBO was less sensitive to microglia- and macrophage-mediated inhibition of viral replication compared with rHSVQ1 (Fig. 2B and C). However, in the presence of a TNFα-blocking antibody, rHSVQ1 replicated as well as RAMBO in glioma cells cultured with BV2 (Fig. 4C). These data suggest that oHSV-infected glioma cells induce murine TNF production by macrophage/microglia, which then suppresses oHSV replication through a paracrine mechanism. The strength of the TNFα response elicited by each virus correlates with its differential viral replication; this explains why RAMBO replicates better than rHSVQ1 in the coculture system. These findings further suggest that Vstat120 expression by RAMBO-infected glioma cells prevents TNFα production by macrophages/microglial cells.

Effect of BAI1 receptor expression on macrophage response to oHSV

Because Vstat120 is the N-terminus of BAI1, and is expressed on macrophages, we reasoned that BAI1 could be involved in instructing an antiviral function in macrophages, and Vstat120

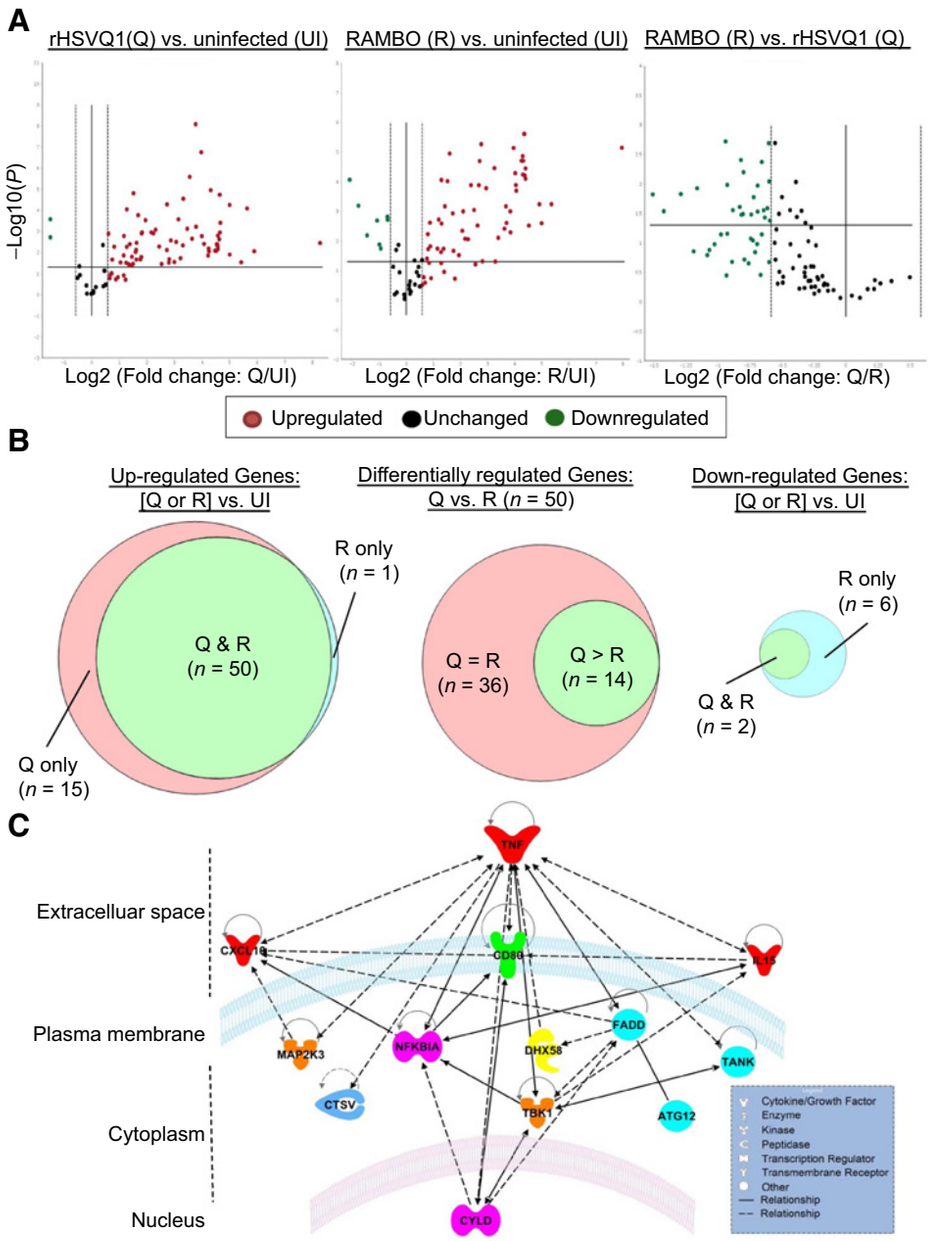

Figure 3.
Changes in anti-viral signaling in macrophages co-cultured with glioma infected with RAMBO versus rHSVQ1. Comparison of murine macrophage anti-viral gene signaling when cultured with rHSVQ1 or RAMBO-infected glioma cells. Briefly, U251 human glioma cells infected with PBS, rHSVQ1, or RAMBO were overlaid with murine RAW macrophage cells. Twelve hours after infection, we analyzed changes in murine-specific cytokine gene expression using an antiviral gene-expression PCR array. **A,** Volcano plot comparing normalized changes in gene expression of macrophages cultured with glioma cells treated with rHSVQ1 versus uninfected (left), RAMBO versus uninfected (middle), and RAMBO versus rHSVQ1 (right) using 1.5-fold gene change as a cut-off value, and $P \leq 0.05$. **B,** Venn diagrams of macrophage genes induced upon infection with rHSVQ1 and/or RAMBO (left), induced by both rHSVQ1 and RAMBO relative to uninfected (middle) and downregulated by rHSVQ1 and/or RAMBO (right). **C,** IPA of genes showing a differentially induction ($\geq$ 1.5-fold) in macrophages in response to rHSVQ1 versus RAMBO-infected cells. The network is graphically represented as nodes (genes); bold lines connecting the nodes indicate direct interaction, whereas the dashed lines suggest indirect interaction.

may function as a decoy receptor. This would result in the negative regulation of BAI1-mediated antiviral signaling. To first test if macrophage expression of BAI1 plays a role in its inflammatory response towards viral infection, we compared the antiviral effects of macrophages derived from *Bai1/Adgrb1*$^{-/-}$ (knockout) or *Bai1*$^{+/+}$ (wild-type) littermate mice. A significant increase in viral gene (ICP4) expression and replication was observed in rHSVQ1-infected human glioma cells cultured with *Bai1*$^{-/-}$ mouse macrophages compared with *Bai1*$^{+/+}$ macrophages (Fig. 5A and B; black bars). This result exposed an antiviral function of *Bai1* that was rescued in macrophages from *Bai1*$^{-/-}$ mice. Viral replication of RAMBO infected cocultures was significantly higher than rHSVQ1 cocultures in the presence of *Bai1*$^{+/+}$ macrophages [Fig. 5A and B; black bars (rHSVQ1) vs. gray bars (RAMBO)]. However, in the presence of *Bai1*$^{-/-}$ macrophages, the increase in ICP4 expression and viral replication was lost [Fig. 5A and B; black bars (rHSVQ1) vs. gray bars (RAMBO)]. These results revealed that although RAMBO tempered antiviral responses mediated by BAI1 in macrophages. The failure of *Bai1*$^{-/-}$ macrophages to antagonize rHSVQ1 replication was accompanied with a significantly reduced *TNFα* gene expression (Fig. 5C). Overall, increased viral gene expression and replication in cocultures with *Bai1*$^{-/-}$ macrophages revealed a role for BAI1 expression in virus clearance.

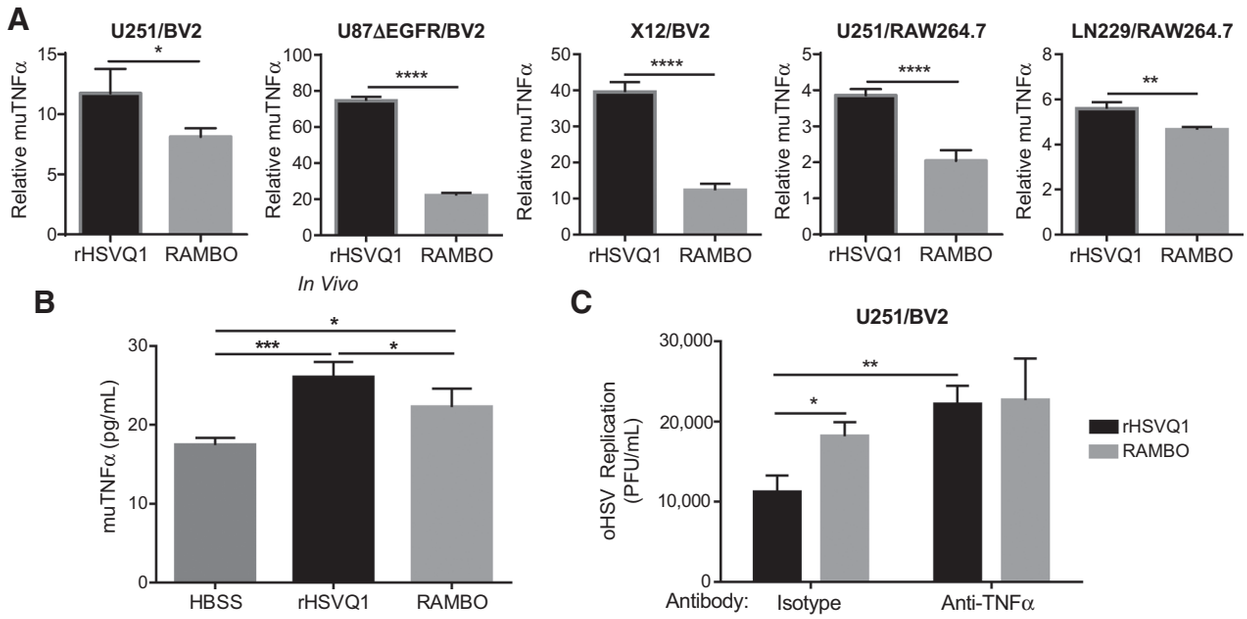

Figure 4.

RAMBO reduces infection-induced TNFα secretion by macrophages and microglia. **A,** Human glioma cells infected ± oHSV (rHSVQ1 or RAMBO) were overlaid with murine macrophages or microglia. Change in murine TNFα gene expression relative to uninfected cocultures was measured 12 hours after overlay of the indicated RAW or BV2 cells (using species-specific primers). Data shown are mean fold-change in gene expression ± SD, normalized to expression without infection (relative expression, normalized to uninfected control; $2^{-\Delta\Delta C_t}$). **B,** Mice bearing intracranial U87ΔEGFR tumors treated with HBSS (inoculation control), rHSVQ1, or RAMBO were sacrificed 3 days after treatment, and tumor-bearing hemispheres were analyzed for muTNFα using ELISA. Data shown are mean muTNFα (pg/mL) ± SD. rHSVQ1 infection resulted in significant increase in muTNFα, compared with uninfected injection control (HBSS). **C,** U251 glioma cells infected with rHSVQ1 or RAMBO were overlaid with BV2 microglia with isotype or TNFα-blocking antibody. Twelve hours later, virus replication was evaluated via standard plaque assay. Data shown are mean replication (plaque-forming U/mL) ± SD (*, $P \leq 0.05$; **, $P \leq 0.01$; ***, $P \leq 0.001$; ****, $P \leq 0.0001$).

RAMBO is safe and effective in immunocompetent models

We next evaluated the importance of BAI1 receptor expression on wild-type HSV-1 infection in the brain. Using *Bai1*$^{-/-}$ mice or wild-type littermates, we intracranially inoculated mice with wild-type F strain HSV-1, and monitored for survival. *Bai1*$^{-/-}$ mice showed significant resistance to HSV1-induced toxicity and survived longer than wild-type littermates (Fig. 5D). These results confirm that BAI1 receptor expression on macrophages plays a significant role in their response to both wild-type and oncolytic HSV therapy. Given the impact of Vstat120 on macrophage response to viral infection, we tested the safety of RAMBO in non–tumor-bearing female BALB/C mice by direct intracranial inoculation of the virus. All mice treated with as little as 1×10^4 pfu of wild type HSV-1 F strain displayed rapid weight loss, neurological symptoms, and met early removal criteria by day 7 mandating their euthanization (Fig. 6A and B). Mice treated with oncolytic RAMBO at a log fold higher dose (1×10^5 pfu) exhibited transient weight loss, but recovered by 7 days after treatment. Collectively, this experiment suggests that while RAMBO tempers the macrophage antiviral response allowing for better virus propagation *in vivo* and increased oncolytic efficacy, it can be safely pursued for clinical development.

Discussion

Angiogenesis is a hallmark of aggressive malignant glioblastoma, and numerous strategies to curb it using antibodies, small-molecule inhibitors, etc., have been tested preclinically and in patients both as single agent and as combination strategies. Evaluation of changes in tumor microenvironment after oHSV therapy have uncovered changes in vascularization post therapy inciting several studies combining virotherapy with vascular disrupting agents and angiogenesis inhibitors (37). We have previously demonstrated increased antitumor effects when arming oHSV with Vstat120, a 120-kDa cleaved secreted fragment of BAI1, against a variety of preclinical cancer models, including glioblastoma, ovarian cancer, and head and neck cancer (6, 32, 38, 39). These effects had been heretofore attributed to the antiangiogenic effect of Vstat120 mediated by its conserved type I thrombospondin type I repeats (TSR), which bind to CD36 on endothelial cells and induce apoptosis (12, 13). Here, we demonstrate that arming an oHSV with Vstat120 also has a shielding effect against macrophages/microglia antiviral responses.

Oncolytic HSV infections in brain tumor models typically generate a robust inflammatory response, leading to massive infiltration of macrophages/microglia in the tumor, which leads to a reduction in the antitumor efficacy of oHSV (29). Our current investigations revealed that brain tumor infection with RAMBO, an oHSV-expressing Vstat120 showed a dramatic reduction in macrophage/microglial infiltrates compared with a control oHSV, rHSVQ1. These results demonstrate that Vstat120 expression in the context of an oHSV counters the inflammatory response towards oHSV. Increased virus propagation accompanied reduced macrophage infiltration into

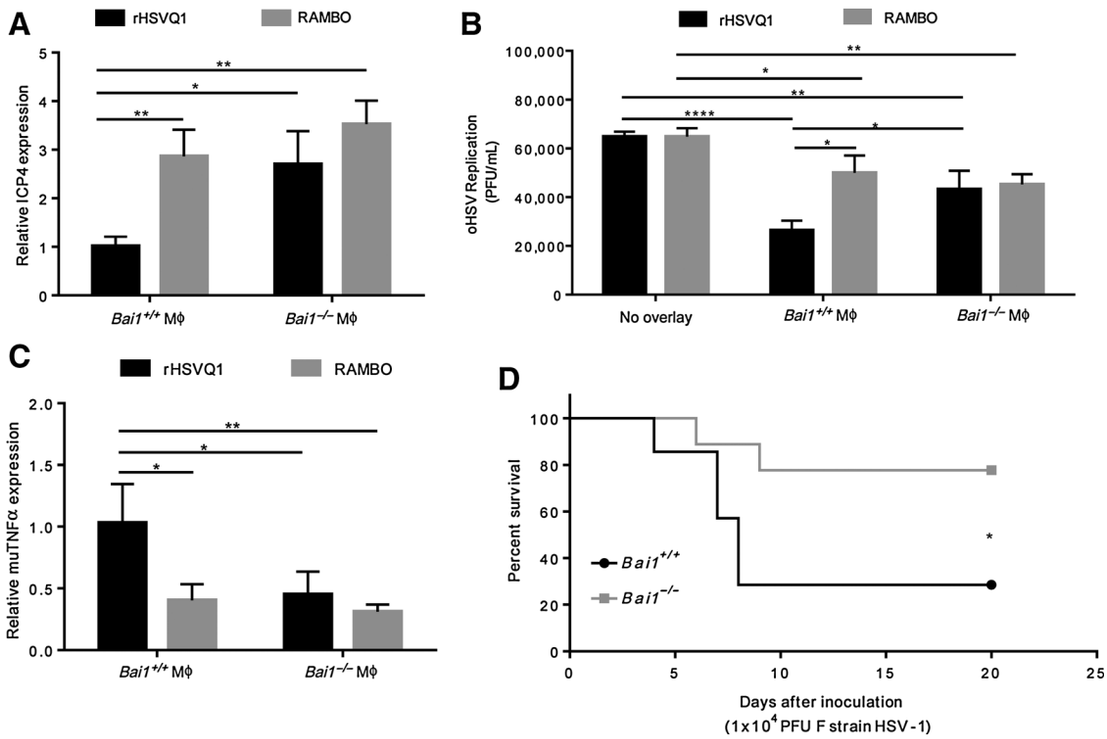

Figure 5.

Reduced TNFα upon RAMBO infection depends on BAI1 expression in macrophages. Primary bone marrow–derived murine macrophages from *Bai1*$^{+/+}$ or *Bai1*$^{-/-}$ mice were used to evaluate the impact of BAI1 on viral replication in coculture with U251 glioma cells. **A,** Twelve hours after infection, changes in viral ICP4 gene expression was compared between rHSVQ1 or RAMBO-infected cells cultured with *Bai1*$^{+/+}$ or *Bai1*$^{-/-}$ macrophages. Data shown are mean fold-change in ICP4 gene expression ± SD, normalized to levels in rHSVQ1/*Bai1*$^{+/+}$ co-culture. **B,** Twelve hours after infection, changes in viral replication was compared between rHSVQ1- or RAMBO-infected U251 glioma cells cultured with *Bai1*$^{+/+}$ or *Bai1*$^{-/-}$ macrophages. Data shown are mean replication (plaque-forming U/mL) ± SD. **C,** Change in murine TNFα gene expression was measured 12 hours after coculture with infected U251 glioma cells. Data shown are relative TNFα gene expression ± SD, normalized to expression in *Bai1*$^{+/+}$ cocultured with rHSVQ1. **D,** Wild-type HSV-1 (F strain) was injected into naïve non–tumor-bearing brains of *Bai1*$^{-/-}$ or *Bai1*$^{+/+}$ mice. Data shown are Kaplan–Meier survival curve. Mice were euthanized when they showed symptoms of viral encephalitis, including hunched posture, rough coat, thin body, or limb paralysis. (*, $P \leq 0.05$; **, $P \leq 0.01$; ****, $P \leq 0.0001$).

tumors treated with RAMBO compared with a control oHSV. In a coculture system, RAMBO-infected glioma cells failed to activate a robust inflammatory cytokine response in macrophages. In particular, there was a strong reduction in TNFα gene expression and secretion by macrophages and microglia. Neutralization of TNFα in the coculture with control oHSV reversed the antiviral response and restored viral replication. These findings reveal TNFα to be a major effector that orchestrates the antiviral response of macrophages/microglia, and that it is antagonized by Vstat120.

BAI1 is known to function as a phagocytic receptor, which contributes to engulfment and clearance of apoptotic cells (14) and Gram-negative bacteria (18, 40). As an engulfment receptor, it functions via recognition and binding to phosphatidyl serine on apoptotic cells and to cell surface LPS of Gram-negative bacteria of infected cells (14, 16, 41) via its thrombospondin type 1 repeats

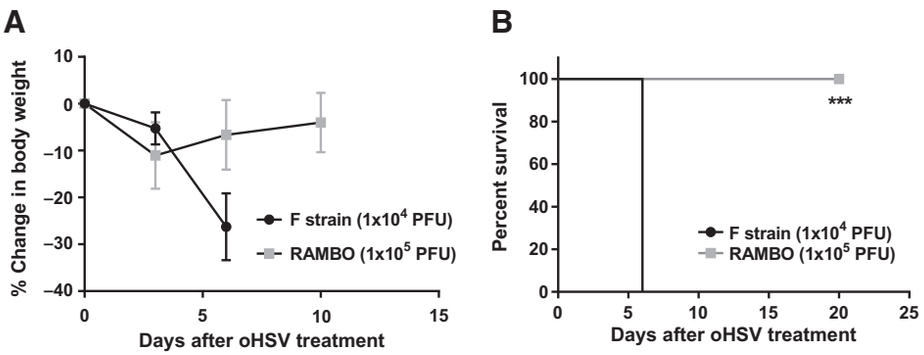

Figure 6.

RAMBO safety in immunocompetent mice. Wild-type HSV-1 (F strain) or RAMBO was injected into naive non–tumor-bearing brains of HSV sensitive female Balb/C mice. **A,** Change in the percentage of body weight of mice inoculated with wild-type F strain HSV-1 or RAMBO. **B,** Kaplan–Meier survival curves of mice inoculated with wild-type F strain HSV-1 or RAMBO. (***, $P \leq 0.001$).

(TSRs), triggering Rac1 activation of ELMO/Doc, resulting in increased phagocytic activity (18). Bai1 knockout mice exhibit impaired anti-microbial activity, and increased susceptibility to bacterial sepsis (40). Here our results show for the first time that, although wild-type primary bone marrow–derived macrophages inhibited oHSV replication in cocultured glioma cells, *Bai1*$^{-/-}$ macrophages were defective in their ability to curb virus replication, implicating an antiviral role for this multifunctional cell surface receptor.

Bai1$^{-/-}$ macrophage deficiency in mounting an antiviral response against infected glioma cells was accompanied by a reduction in TNFα induction, mechanistically linking it to Vstat120's effects. Along with the reduced TNFα, *Bai1*$^{-/-}$ mice were also more resistant to virus-induced pathology, corroborating the role of BAI1 in mediating inflammation in response to HSV-1 in the brain. Collectively, these results support a model whereby Vstat120 expression can inhibit TNFα production by blocking BAI1-mediated macrophage response to viral infection, and thus increase oHSV propagation in tumors. How Vstat120 might block the function of BAI1 in macrophage response to infected tumor cells is currently unclear, but we can envision two likely mechanisms. The first is a dominant negative competition model that assumes the extracellular domain of BAI1 is actively involved in the recognition of infected cells, likely through its TSRs. Vstat120 could shield infected tumor cells from macrophages/microglia by saturating all the BAI1-binding sites on the tumor cells. In the second model, Vstat120's inhibitory action would occur directly on the macrophages/microglia. It has been shown that the cleaved extracellular domains of adhesion GPCRs stay associated with the 7-transmembrane region of the cleaved receptor, and act as antagonists (42). Detachment of the N-terminal fragment from the cleaved receptor activates receptor signaling. In this fashion, it is conceivable that Vstat120 might dampen a signal necessary for the macrophage antiviral response. This second model also differs from the first one in that it does not assume that BAI1 is the prime sensor of the presence of infected cells by macrophages, it could also function in a costimulatory role.

Further investigations are warranted to determine whether BAI1 recognizes infected cells through a mechanism similar to its ability to clear bacterially infected or apoptotic cells. It is possible that TSRs serve as recognition modules for a variety of pathogens. TSR are quite diverse in sequence, and the five TSRs in BAI1 share homology, but are not identical, suggesting that each TSR might confer the protein with unique substrate recognition abilities. Further studies with mutations in the individual TSRs of Vstat120 will help define their roles in the anti-inflammatory response. The signaling pathway that might trigger alterations in cytokine expression downstream of BAI1 remains to be identified. BAI1 can signal via several G-protein–dependent and independent pathways. It can activate small G proteins of the Gα12/13, as well as signal via Elmo/Dock/Ras or activate Erk signaling (43).

TNFα has been confirmed by multiple studies to play a critical role in tumor cell migration invasion, proliferation, and angiogenesis. In addition, it is considered to be the major cytokine involved in cachexia, as well as systemic toxicity in patients. Consistent with this an oHSV encoding for TNFα was shown to increase systemic toxicity with no therapeutic advantage over control virus (44). Thus, the reduction of TNFα in the context of virotherapy is of high potential significance. Although long-term abrogation of TNFα (such as in *TNFα*$^{-/-}$ mice) has been associated with increased risk of wild-type HSV-1 infection (45), transient blockade of TNFα along with anti-herpetic agents significantly increased the survival rate of mice inoculated with HSV-1 (46). These results support the involvement of inflammation in the pathogenesis of HSV-induced encephalitis, and efforts to combined HSV therapy with TNFα inhibition can be a useful approach for oncolytic virus treatment. Consistent with this idea, we have previously shown that blockade of TNFα with a blocking antibody in mice bearing tumors led to increased virus replication and antitumor efficacy (22). Our study further shows that along with the moderation of TNFα and the resulting increased oHSV propagation in tumors, Vstat1 20-expressing oHSV remains safe at clinically relevant doses upon intracranial inoculation in non–tumor-bearing mice. These studies encourage the further development of Vstat120-expressing oHSV as a therapeutic strategy to improve outcome for brain tumor patients.

Disclosure of Potential Conflicts of Interest

E.G. Van Meir is listed as a co-inventor on a patent, which is owned by Emory University, on method of treating abnormal angiogenesis via the BAI family of proteins and their protein fragments. No potential conflicts of interest were disclosed by the other authors.

Authors' Contributions

Conception and design: C. Bolyard, W.H. Meisen, C. Alvarez-Breckenridge, P. Pow-anpongkul, M.A. Caligiuri, J. Yu, B. Kaur

Development of methodology: C. Bolyard, W.H. Meisen, Y. Banasavadi-Siddegowda, J. Hardcastle, J.Y. Yoo, E.S. Wohleb, J.-G. Yu, C. Alvarez-Breckenridge, P. Pow-anpongkul, F. Pichiorri, J.P. Godbout

Acquisition of data (provided animals, acquired and managed patients, provided facilities, etc.): C. Bolyard, W.H. Meisen, Y. Banasavadi-Siddegowda, J. Hardcastle, J.Y. Yoo, E.S. Wohleb, J. Wojton, J.-G. Yu, S. Dubin, J. Smith, M. Old, D. Zhu, E.G. Van Meir, J.P. Godbout

Analysis and interpretation of data (e.g., statistical analysis, biostatistics, computational analysis): C. Bolyard, W.H. Meisen, Y. Banasavadi-Siddegowda, J. Hardcastle, J.Y. Yoo, J. Wojton, M. Khosla, P. Pow-anpongkul, J. Zhang, E.G. Van Meir, J.P. Godbout, M.A. Caligiuri

Writing, review, and/or revision of the manuscript: C. Bolyard, W.H. Meisen, E.S. Wohleb, M. Old, E.G. Van Meir, J.P. Godbout, J. Yu, B. Kaur

Administrative, technical, or material support (i.e., reporting or organizing data, constructing databases): C. Bolyard, B. Xu

Study supervision: C. Bolyard, M. Old, M.A. Caligiuri, J. Yu, B. Kaur

Acknowledgments

We would like to acknowledge the Analytical Cytometry Shared Resource, the Center for Biostatistics, and the Target Validation Shared Resources within the James Comprehensive Cancer Center, all at The Ohio State University, for their services. We also acknowledge creative commons (https://creativecommons.org/licenses/by/3.0/) whose material was used to create cartoons in Figure 2.

Grant Support

This work is supported in part by: NIH grants R01NS064607, R01CA150153, P30NS045758 (to B. Kaur); P01CA163205 (to B. Kaur and M.A. Caligiuri), Pelotonia Fellowship (to S. Dubin); T32CA009338 (to C. Bolyard), IRG-67-003-50 (to J.Y. Yoo), P30CA016058 (to M.A. Caligiuri and B. Kaur), R01NS096236, P30CA138292, the Southeastern Brain Tumor Foundation (to E.G. Van Meir) and the CURE Childhood Cancer and St. Baldrick's Foundations (to E.G. Van Meir and D. Zhu).

The costs of publication of this article were defrayed in part by the payment of page charges. This article must therefore be hereby marked *advertisement* in accordance with 18 U.S.C. Section 1734 solely to indicate this fact.

Received July 19, 2016; revised October 4, 2016; accepted October 27, 2016; published OnlineFirst November 9, 2016.

References

1. Ahmed AU, Auffinger B, Lesniak MS. Understanding glioma stem cells: rationale, clinical relevance and therapeutic strategies. Expert Rev Neurother 2013;13:545–55.
2. Wojton J, Meisen WH, Kaur B. How to train glioma cells to die: molecular challenges in cell death. J Neurooncol 2016;126:377–84.
3. Veerapong J, Bickenbach KA, Shao MY, Smith KD, Posner MC, Roizman B, et al. Systemic delivery of (gamma1)34.5-deleted herpes simplex virus-1 selectively targets and treats distant human xenograft tumors that express high MEK activity. Cancer Res 2007; 67:8301–6.
4. Dmitrieva N, Yu L, Viapiano M, Cripe TP, Chiocca EA, Glorioso JC, et al. Chondroitinase ABC I-mediated enhancement of oncolytic virus spread and antitumor efficacy. Clin Cancer Res 2011;17: 1362–72.
5. Andtbacka RH, Kaufman HL, Collichio F, Amatruda T, Senzer N, Chesney J, et al. Talimogene laherparepvec improves durable response rate in patients with advanced melanoma. J Clin Oncol 2015;33:2780–8.
6. Hardcastle J, Kurozumi K, Dmitrieva N, Sayers MP, Ahmad S, Waterman P, et al. Enhanced antitumor efficacy of vasculostatin (Vstat120) expressing oncolytic HSV-1. Mol Ther 2010;18:285–94.
7. Fukushima Y, Oshika Y, Tsuchida T, Tokunaga T, Hatanaka H, Kijima H, et al. Brain-specific angiogenesis inhibitor 1 expression is inversely correlated with vascularity and distant metastasis of colorectal cancer. Int J Oncol 1998;13:967–70.
8. Hatanaka H, Oshika Y, Abe Y, Yoshida Y, Hashimoto T, Handa A, et al. Vascularization is decreased in pulmonary adenocarcinoma expressing brain-specific angiogenesis inhibitor 1 (BAI1). Int J Mol Med 2000; 5:181–3.
9. Kaur B, Brat DJ, Calkins CC, Van Meir EG. Brain angiogenesis inhibitor 1 is differentially expressed in normal brain and glioblastoma independently of p53 expression. Am J Pathol 2003;162:19–27.
10. Lee JH, Koh JT, Shin BA, Ahn KY, Roh JH, Kim YJ, et al. Comparative study of angiostatic and anti-invasive gene expressions as prognostic factors in gastric cancer. Int J Oncol 2001;18:355–61.
11. Wang W, Da R, Wang M, Wang T, Qi L, Jiang H, et al. Expression of brain-specific angiogenesis inhibitor 1 is inversely correlated with pathological grade, angiogenesis and peritumoral brain edema in human astrocytomas. Oncol Lett 2013;5:1513–8.
12. Klenotic PA, Huang P, Palomo J, Kaur B, Van Meir EG, Vogelbaum MA, et al. Histidine-rich glycoprotein modulates the anti-angiogenic effects of vasculostatin. Am J Pathol 2010;176:2039–50.
13. Kaur B, Cork SM, Sandberg EM, Devi NS, Zhang Z, Klenotic PA, et al. Vasculostatin inhibits intracranial glioma growth and negatively regulates *in vivo* angiogenesis through a CD36-dependent mechanism. Cancer Res 2009;69:1212–20.
14. Park D, Tosello-Trampont AC, Elliott MR, Lu M, Haney LB, Ma Z, et al. BAI1 is an engulfment receptor for apoptotic cells upstream of the ELMO/Dock180/Rac module. Nature 2007;450:430–4.
15. Sokolowski JD, Nobles SL, Heffron DS, Park D, Ravichandran KS, Mandell JW. Brain-specific angiogenesis inhibitor-1 expression in astrocytes and neurons: implications for its dual function as an apoptotic engulfment receptor. Brain Behav Immun 2011;25:915–21.
16. Harre U, Keppeler H, Ipseiz N, Derer A, Poller K, Aigner M, et al. Moonlighting osteoclasts as undertakers of apoptotic cells. Autoimmunity 2012;45:612–9.
17. Elliott MR, Zheng S, Park D, Woodson RI, Reardon MA, Juncadella IJ, et al. Unexpected requirement for ELMO1 in clearance of apoptotic germ cells *in vivo*. Nature 2010;467:333–7.
18. Das S, Owen KA, Ly KT, Park D, Black SG, Wilson JM, et al. Brain angiogenesis inhibitor 1 (BAI1) is a pattern recognition receptor that mediates macrophage binding and engulfment of Gram-negative bacteria. Proc Natl Acad Sci U S A 2011;108:2136–41.
19. Alvarez-Breckenridge CA, Yu J, Price R, Wojton J, Pradarelli J, Mao H, et al. NK cells impede glioblastoma virotherapy through NKp30 and NKp46 natural cytotoxicity receptors. Nat Med 2012;18:1827–34.
20. Haralambieva I, Iankov I, Hasegawa K, Harvey M, Russell SJ, Peng KW. Engineering oncolytic measles virus to circumvent the intracellular innate immune response. Mol Ther 2007;15:588–97.
21. Ikeda K, Ichikawa T, Wakimoto H, Silver JS, Deisboeck TS, Finkelstein D, et al. Oncolytic virus therapy of multiple tumors in the brain requires suppression of innate and elicited antiviral responses. Nat Med 1999; 5:881–7.
22. Meisen WH, Wohleb ES, Jaime-Ramirez AC, Bolyard C, Yoo JY, Russell L, et al. The impact of macrophage- and microglia-secreted TNFalpha on oncolytic HSV-1 therapy in the glioblastoma tumor microenvironment. Clin Cancer Res 2015;21:3274–85.
23. Wakimoto H, Johnson PR, Knipe DM, Chiocca EA. Effects of innate immunity on herpes simplex virus and its ability to kill tumor cells. Gene Ther 2003;10:983–90.
24. Peng KW, Myers R, Greenslade A, Mader E, Greiner S, Federspiel MJ, et al. Using clinically approved cyclophosphamide regimens to control the humoral immune response to oncolytic viruses. Gene therapy 2013;20: 255–61.
25. Currier MA, Gillespie RA, Sawtell NM, Mahller YY, Stroup G, Collins MH, et al. Efficacy and safety of the oncolytic herpes simplex virus rRp450 alone and combined with cyclophosphamide. Mol Ther 2008;16:879–85.
26. Qiao J, Wang H, Kottke T, White C, Twigger K, Diaz RM, et al. Cyclophosphamide facilitates antitumor efficacy against subcutaneous tumors following intravenous delivery of reovirus. Clin Cancer Res 2008; 14:259–69.
27. Lun XQ, Jang JH, Tang N, Deng H, Head R, Bell JC, et al. Efficacy of systemically administered oncolytic vaccinia virotherapy for malignant gliomas is enhanced by combination therapy with rapamycin or cyclophosphamide. Clin Cancer Res 2009;15:2777–88.
28. Haseley A, Boone S, Wojton J, Yu L, Yoo JY, Yu J, et al. Extracellular matrix protein CCN1 limits oncolytic efficacy in glioma. Cancer Res 2012;72: 1353–62.
29. Thorne AH, Meisen WH, Russell L, Yoo JY, Bolyard CM, Lathia JD, et al. Role of cysteine-rich 61 protein (CCN1) in macrophage-mediated oncolytic herpes simplex virus clearance. Mol Ther 2014;22:1678–87.
30. Otsuki A, Patel A, Kasai K, Suzuki M, Kurozumi K, Chiocca EA, et al. Histone deacetylase inhibitors augment antitumor efficacy of herpes-based oncolytic viruses. Mol Ther 2008;16:1546–55.
31. Terada K, Wakimoto H, Tyminski E, Chiocca EA, Saeki Y. Development of a rapid method to generate multiple oncolytic HSV vectors and their *in vivo* evaluation using syngeneic mouse tumor models. Gene Ther 2006;13: 705–14.
32. Yoo JY, Haseley A, Bratasz A, Chiocca EA, Zhang J, Powell K, et al. Antitumor efficacy of 34.5ENVE: a transcriptionally retargeted and "Vstat120"-expressing oncolytic virus. Mol Ther 2012;20:287–97.
33. Zhu D, Li C, Swanson AM, Villalba RM, Guo J, Zhang Z, et al. BAI1 regulates spatial learning and synaptic plasticity in the hippocampus. J Clin Invest 2015;125:1497–508.
34. Fang H, Pengal RA, Cao X, Ganesan LP, Wewers MD, Marsh CB, et al. Lipopolysaccharide-induced macrophage inflammatory response is regulated by SHIP. J Immunol 2004;173:360–6.
35. Henry CJ, Huang Y, Wynne A, Hanke M, Himler J, Bailey MT, et al. Minocycline attenuates lipopolysaccharide (LPS)-induced neuroinflammation, sickness behavior, and anhedonia. J Neuroinflammation 2008;5:15.
36. Huang Y, Henry CJ, Dantzer R, Johnson RW, Godbout JP. Exaggerated sickness behavior and brain proinflammatory cytokine expression in aged mice in response to intracerebroventricular lipopolysaccharide. Neurobiol Aging 2008;29:1744–53.
37. Kaur B, Chiocca EA, Cripe TP. Oncolytic HSV-1 virotherapy: clinical experience and opportunities for progress. Curr Pharm Biotechnol 2012; 13:1842–51.
38. Yoo JY, Yu JG, Kaka A, Pan Q, Kumar P, Kumar B, et al. ATN-224 enhances antitumor efficacy of oncolytic herpes virus against both local and metastatic head and neck squamous cell carcinoma. Mol Ther Oncolytics 2015;2:15008.
39. Bolyard C, Yoo JY, Wang PY, Saini U, Rath KS, Cripe TP, et al. Doxorubicin synergizes with 34.5ENVE to enhance antitumor efficacy against metastatic ovarian cancer. Clin Cancer Res 2014;20:6479–94.
40. Billings EA, Lee CS, Owen KA, D'Souza RS, Ravichandran KS, Casanova JE. The adhesion GPCR BAI1 mediates macrophage ROS production and microbicidal activity against Gram-negative bacteria. Sci Signal 2016;9: ra14.
41. Das S, Sarkar A, Ryan KA, Fox S, Berger AH, Juncadella IJ, et al. Brain angiogenesis inhibitor 1 is expressed by gastric phagocytes during

infection with Helicobacter pylori and mediates the recognition and engulfment of human apoptotic gastric epithelial cells. FASEB J 2014; 28:2214–24.
42. Kishore A, Purcell RH, Nassiri-Toosi Z, Hall RA. Stalk-dependent and stalk-independent signaling by the adhesion G protein-coupled receptors GPR56 (ADGRG1) and BAI1 (ADGRB1). J Biol Chem 2016;291: 3385–94.
43. Stephenson JR, Purcell RH, Hall RA. The BAI subfamily of adhesion GPCRs: synaptic regulation and beyond. Trends Pharmacol Sci 2014;35: 208–15.
44. Han ZQ, Assenberg M, Liu BL, Wang YB, Simpson G, Thomas S, et al. Development of a second-generation oncolytic Herpes simplex virus expressing TNFalpha for cancer therapy. J Gene Med 2007;9:99–106.
45. Sergerie Y, Rivest S, Boivin G. Tumor necrosis factor-alpha and interleukin-1 beta play a critical role in the resistance against lethal herpes simplex virus encephalitis. J Infect Dis 2007;196:853–60.
46. Boivin N, Menasria R, Piret J, Rivest S, Boivin G. The combination of valacyclovir with an anti-TNF alpha antibody increases survival rate compared to antiviral therapy alone in a murine model of herpes simplex virus encephalitis. Antiviral Res 2013;100:649–53.